



Journal Name

COMMUNICATION

Triply green polyaniline: UV irradiation-induced synthesis of highly porous PANI/TiO₂ composite and its application in dye removal

Received 00th January 20xx,
Accepted 00th January 20xx

DOI: 10.1039/x0xx00000x

www.rsc.org/

Carolina Cionti,^{a,b} Cristina Della Pina,^{a,c} Daniela Meroni,^{*,a,b} Ermelinda Falletta,^{*,a,c} and Silvia Ardizzone^{a,b}

An environmental benign procedure for the preparation of polyaniline/TiO₂ composites is presented. The UV irradiation-induced synthesis leads to materials with good crystallinity and tailored morphology, showing promising sorption and recycle properties in dye removal tests. A reaction mechanism is proposed on the basis of LC-MS and FT-IR investigations.

Polyaniline (PANI) is a prominent member of the organic conducting polymer family, which has a broad range of applications ranging from electronics, optics and photovoltaics.¹⁻⁴ Moreover, PANI has recently received increasing attention as an alternative sorbent for pollutant removal, able to replace activated carbon.⁵⁻⁷ In this respect, PANI does not require energy-consuming thermal activation and regeneration treatments. Generally, the synthesis of PANI involves the oxidative polymerization of aniline by strong oxidants (*e.g.*, peroxydisulfates) in stoichiometric amount⁸ (labelled in the text as PANI1). Besides the use of noxious reagents, the classical synthetic approach also leads to toxic, carcinogenic and mutagenic byproducts (benzidine and trans-azobenzene) as well as to large amounts of inorganic coproducts (typically sulphates), which necessitate extensive purification producing a high volume of waste. More environmental friendly alternatives have been proposed using benign reagents such as the aniline dimer (*N*-(4-aminophenyl) aniline) and H₂O₂.⁹⁻¹² In particular, some of us have previously reported¹³ a green method consisting in the Fe³⁺-catalyzed oxidative polymerization of the dimer by H₂O₂ (named PANI2 in the following). This innovative approach leads to water as only co-product and completely eliminates toxic by-products, simplifying the polymer post-treatment. However, in this case, the control of the morphological features of the polymer is more challenging, resulting in materials with poor sorption capability.

Here, we report for the first time an innovative UV irradiation-induced synthetic procedure for the preparation of PANI with tailored morphological features, starting from green reactants. The process is activated by semiconducting TiO₂, leading to composites (PANI_TiO₂) with high surface area and porosity, which were successfully adopted as sorbents for the removal of dyes from aqueous matrix. For the remediation tests, methyl orange (MO), a model for anionic azo dyes, was selected as target pollutant due to its eco-toxicity and potential bioaccumulation dangers.¹⁴ Moreover, a green regeneration procedure by water was developed to recover the dye and restore the PANI sorbent properties.

Figure 1a shows a schematic illustration of PANI growth on TiO₂ during the composite preparation. Details of the experimental procedure for the materials preparation and characterization are given in the supplementary information. The reaction mechanism can be described as a two steps process: 1) UV-mediated PANI oligomers growth on the TiO₂ surface, 2) oligomers polymerization by H₂O₂. In order to elucidate the reaction mechanism involved in the PANI_TiO₂ formation, LC-MS analyses were carried out on the liquid part of the reaction mixture collected at different times, whereas FT-IR analyses were simultaneously conducted on the solid separated from the solution. LC-MS analyses did not show the presence of oligomers or intermediates in the liquid phase during PANI preparation; only the starting unreacted *N*-(4-aminophenyl) aniline was detected (Figure 1c). On the contrary, FT-IR analyses (Figure 1d) clearly show the growth of the polymer on the TiO₂ surface during UV irradiation, which supports radicals production at the surface of the TiO₂ photocatalyst¹⁵. This is confirmed by the intensity increase of the bands at around 1500 and 1580 cm⁻¹, assigned to the C=C stretching of the benzene and quinoid rings respectively, at about at 1310 cm⁻¹ and 1245 cm⁻¹, related to C-N and C=N stretching modes, and at *ca.* 1028 cm⁻¹, typical of in-plane and out-of-plane C-N bending vibrations. Moreover, the growing broad band in the range 2500-3500 cm⁻¹ guarantees the presence of a more extended conjugation along the oligomeric chains after longer irradiation time. However, the typical green PANI polymer in the form of emeraldine salt (Fig. S1, ESI) was obtained only after the addition of the oxidizing agent (H₂O₂), giving a final yield of 90%. H₂O₂ plays an essential role in the PANI_TiO₂ synthesis since the reaction mechanism is a radical but also oxidative process.

^a Dpt. of Chemistry, Università degli Studi di Milano, via Golgi 19, 20133 Milano, Italy. Email: ermelinda.falletta@unimi.it; daniela.meroni@unimi.it

^b Consorzio INSTM, via Giusti 9, 50121 Florence, Italy.

^c ISTM-CNR, via Golgi 19, 20133 Milano, Italy.

Electronic Supplementary Information (ESI) available: Materials and methods; UV-vis spectrum of PANI_TiO₂; isoelectric point determinations; FTIR spectra of bare TiO₂ and intermediates of PANI_TiO₂noUV; surface area and porosity; XRPD patterns of selected samples. See DOI: 10.1039/x0xx00000x

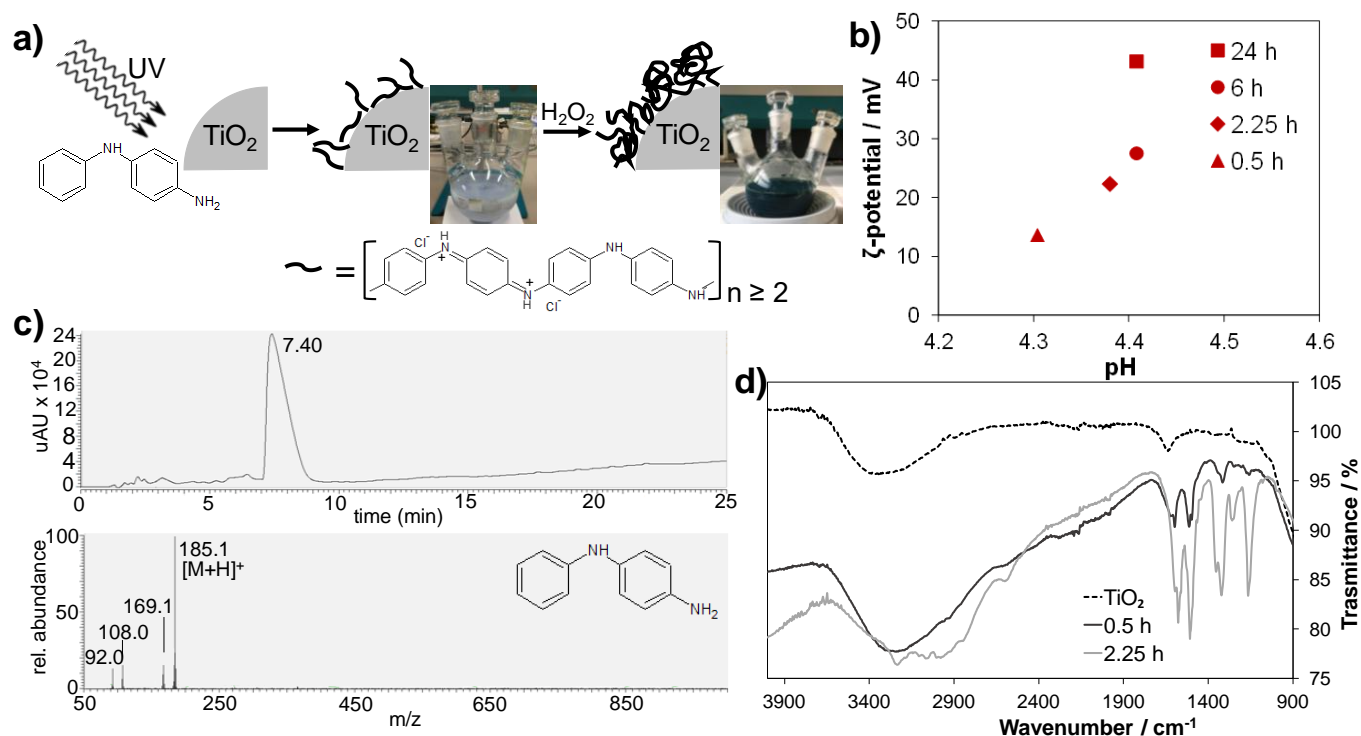


Figure 1. Synthesis of $\text{PANI}_{\text{TiO}_2}$: a) proposed reaction mechanism; b) ζ -potential measurements at spontaneous pH of the product isolated upon irradiation for different time lengths, prior to the addition of H_2O_2 ; c) LC-MS analysis of the supernatant after 2.25 h of UV irradiation and before H_2O_2 addition; d) FTIR spectra of products sampled at different time lengths of irradiation; the spectra of pristine TiO_2 is compared as reference.

TiO_2 has an isoelectric point at pH around 6 (Fig. S2, ESI), therefore in the synthesis acidic conditions the oxide surface is positively charged ($\text{TiOH} + \text{H}^+ = \text{TiOH}_2^+$) and able to adsorb electron donors¹⁶, such as $N-(4\text{-aminophenyl})\text{aniline}$ that in the reaction conditions is

only half-salified (molar ratio reagent/ HCl = 1). This is confirmed by zeta potential experiments of the reaction products sampled at increasing time lengths from the start of the UV irradiation, before the H_2O_2 addition (Figure 1b). At very short reaction times, the free

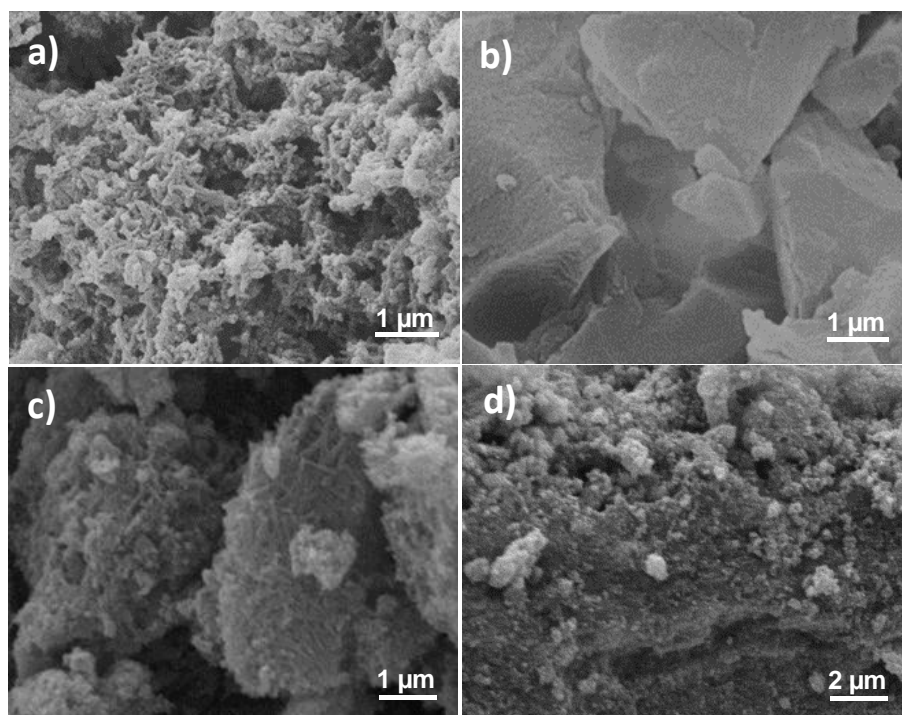


Figure 2. SEM images of PANI1 (a), PANI2 (b), $\text{PANI}_{\text{TiO}_2}$ (c) and $\text{PANI}_{\text{TiO}_2\text{noUV}}$ (d).

charges at the TiO₂ surface, due to the protonation of the surface -OH groups, are partially "inactivated" possibly due to a large coverage by the reactant dimers. At increasing reaction times, the surface of the oxide is the locus of specific adsorption of cationic species from the reaction medium, possibly as a result of oligomerization, leading to an alkaline shift of the isoelectric point (Figure S2, ESI). In order to evaluate the photocatalytic activity of TiO₂ during this step of reaction, similar experiments were conducted in the absence of UV irradiation (sample labelled as PANI_TiO₂noUV) as well as without TiO₂ (PANI_noTiO₂). FT-IR analyses (Figure S3, ESI) revealed that in the absence of UV irradiation, even though *N*-(4-aminophenyl) aniline is adsorbed on the oxide surface, only short oligomers lacking proper conjugation along the chains are produced before H₂O₂ addition, as confirmed by the absence of the broad band between 2500-3500 cm⁻¹, characteristic of extended conjugation. However, also in this case the addition of H₂O₂ leads to a green polymer (PANI_TiO₂noUV), characterized as polyaniline in its emeraldine salt, although in much lower yields (25%). The test without TiO₂ addition leads instead to very poor yields (<5%).

All composite materials were extensively characterized in order to detect any differences ascribable to the reaction mechanism involved. SEM images (Figure 2) show that PANI_TiO₂ presents a highly organized nanorod-based morphology, which results in a high surface area (Figure S4, ESI) and porosity (Figure S5, ESI). It is worth noting that only PANI1 competes with PANI_TiO₂ in terms of surface area, presenting a porous coral-like morphology, whereas PANI2 displays a compact morphology and low surface area. In the case of PANI_TiO₂noUV (Fig. 2d), a more irregular morphology is appreciable, lacking the texture of PANI_TiO₂.

XRPD patterns (Figure 3) of both PANI1 and PANI2 can be attributed to the ES-I form of emeraldine salt¹⁷, which is generally observed when the polymer is obtained from solution in protonated form. The diffraction patterns of PANI_TiO₂ and PANI_TiO₂noUV differ substantially as they contain also the typical diffraction peaks of anatase and rutile TiO₂, in full agreement with the XRPD pattern of the TiO₂ precursor (Figure S6, ESI). Moreover, both XRPD patterns exhibit the presence of much more crystalline ES-I emeraldine with respect to both PANI1 and PANI2, as appreciable from the better resolved peaks and absence of amorphous halo. The PANI_TiO₂noUV presents a much lower PANI content with respect to PANI_TiO₂, as shown by the intensity ratio of the main peaks of the TiO₂ and PANI phases. PANI_noTiO₂ (Figure S7, ESI) displays a comparable PANI pattern.

As reported in the literature¹⁸, the oxidative polymerization reaction of aniline and its derivatives is a fast radical reaction that, if not properly controlled, can promote side-reactions leading to branched and/or overoxidised polymers that negatively affect PANI quality (e.g., morphology, conductivity, porosity). During PANI1 synthesis, the control of the polymer chain growth is ensured by the low reaction temperature, enabling a thermodynamic control of the chain orientation. When *N*-(4-aminophenyl) aniline is used as the reagent, the oxidative polymerization reaction speeds up. The minimum potential value needed to oxidize this compound is 0.80 V, much lower than the one required for aniline (1.05 V).¹⁸⁻²¹ As a consequence, the only temperature monitoring is not sufficient to control and orient the chain growth. As described above for the PANI_TiO₂ synthesis, during the first step of the

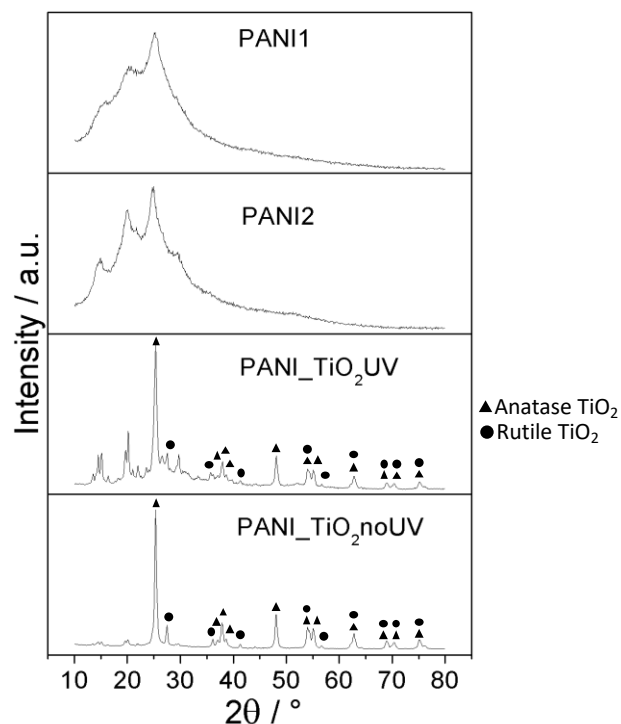


Figure 3. XRPD patterns of the investigated samples.

reaction the synergistic effect of TiO₂ and UV irradiation leads to the growth of PANI oligomers at the oxide surface having the typical structure of the final polymer and, therefore, able to drive the subsequent growth of the chains after oxidant addition. As a consequence, the final material exhibits an organized morphology and improved crystallinity. On the contrary, if the first step of the reaction is not UV-mediated (PANI_TiO₂noUV), the oligomers coated on the inorganic surface are too short. They do not exhibit a chemical structure similar to that of the corresponding final polymer. Therefore, they are less efficient in the promotion of the polymer growth, leading to a final material characterized by an irregular morphology and with lower reaction yield.

Finally, the molecular weight of dimethylformamide soluble PANI_TiO₂ fraction was estimated by SEC using polystyrene standards, obtaining $M_w = 2.8 \times 10^6$ Da (polydispersity about 1.0). These data must be considered as apparent molecular weights and not absolute ones, because polystyrene and PANI have different hydrodynamic volumes.²² However, with respect to previous results on differently synthesized PANI2s^{13,23}, the present innovative synthetic protocol appears to promote the growth of longer chains. All the composites were tested as sorbents for MO removal from aqueous matrices. Experimental details are reported in the supplementary information. Figure 4 reports as in inset the MO percentage removed after 20 minutes contact time. As expected, the materials morphology plays a key role in the dye removal. The samples with the largest surface area (PANI1 and PANI_TiO₂) reveal excellent activity in MO sorption, whereas the PANI2 compact morphology lower the pollutant sorption. No direct relations between the reaction yield and the sorption performance of the sample were observed, see e.g. the comparison between PANI_TiO₂UV and PANI_TiO₂noUV.

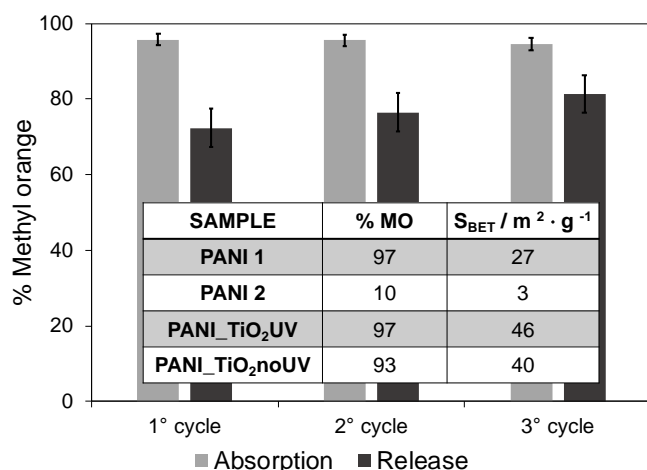


Figure 4. Sorption/release cycles of MO (50 ppm) by PANI_TiO₂. Inset: Sorption data of the different samples together with their relative surface area.

Indeed, the dye removal mechanism is based on anion exchange (Cl⁻ of emeraldine salt vs. dye) and on the formation of interactions between the dyes and the -NH⁺ groups of the emeraldine salt, favoured by a higher accessible surface area. As a result, PANI_TiO₂UV can be successfully applied to the removal of different molecules belonging to the class of anionic azo dyes, as shown by preliminary tests on methyl red.

In order to reduce waste production and process costs the possibility to regenerate and reuse adsorbent materials is crucial. Figure 4 reports recycle tests performed on PANI_TiO₂ using only aqueous solutions for the dye release in order to avoid unfriendly solvents. The composite exhibit a very promising recycling stability, showing totally comparable activity in all the performed tests.

Conclusions

A green procedure has been developed for the synthesis of PANI/TiO₂ composites, using no toxic reagents compared to the conventional PANI synthetic approach. A two-step synthetic procedure provides a more precise control over the oligomerization step, enabling a tailoring of the material properties. Photocatalytic reactions promote the formation of oligomers at the surface of TiO₂, supporting the further growth of polymer chains which occurs only after the addition of H₂O₂. Consequently, a lower amount of H₂O₂ is required with respect to previous works¹³, enabling a stricter control of the final properties of the material. Actually, the present PANI_TiO₂ shows a more ordered morphology and an increased degree of crystallinity. Remediation tests with respect to aqueous dye solutions showed optimal sorption properties and reusability, enabling an easy and green dye retrieval. The use of a heterogeneous photocatalyst opens the door to further enticing applications, such as pollutant removal by combined sorption and photocatalytic oxidation. Further work will exploit this two-step reaction mechanism to further engineer the composite properties for a wealth of possible applications, where high crystallinity and organized morphologies are required.

Conflicts of interest

There are no conflicts to declare.

Notes and references

- C.O. Baker, X. Huang, W. Nelson, R.B. Kaner, *Chem. Soc. Rev.*, 2017, **46**, 1510.
- P. Jiménez, E. Levillain, O. Alévêque, D. Guyomard, B. Lestriez, J. Gaubicher, *Angew. Chem. Int. Ed.*, 2017, **56**, 1553.
- J. Zhang, Z. Zhao, Z. Xia, L. Dai, *Nat. Nanotechnol.*, 2015, **10**, 444.
- F. Cui, Y. Huang, L. Xu, Y. Zhao, J. Lian, J. Bao, H. Li, *Chem. Commun.*, 2018, **54**, 4160.
- J.J. Alcaraz-Espinoza, A.E. Chávez-Guajardo, J.C. Medina-Llamas, C.A.S. Andrade, C.P. De Melo, *ACS Appl. Mater. Interfaces*, 2015, **7**, 7231.
- T. Zhang, X. Huang, T. Asefa, *Chem. Commun.*, 2015, **51**, 16135.
- C. Della Pina, M. A. De Gregorio, L. Clerici, P. Dellavedova, E. Falletta, *J. Hazard. Mater.*, **344**, 2018, 1.
- J. Huang, R.B. Kaner, *Chem. Commun.*, 2006, **0**, 367.
- S.P. Surwade, S.R. Agnihotra, V. Dua, N. Manohar, S. Jain, S. Ammu, S.K. Manohar, *J. Am. Chem. Soc.*, 2009, **131**, 12528.
- Z. Chen, C. Della Pina, E. Falletta, M. Rossi, *J. Catal.*, **367**, 2009, 93.
- H.V. Rasika Dias, X. Wang, R.M. Gamini, Rajapakse, R.L. Elsenbaumer, *Chem. Commun.*, 2006, **0**, 976.
- C. Della Pina, A. M. Ferretti, A. Ponti, E. Falletta, *Compos. Sci. Technol.*, 2015, **110**, 138.
- R. Castagna, M. Tunesi, B. Saglio, C. Della Pina, A. Sironi, D. Albani, C. Bertarelli, E. Falletta, *J. Appl. Polym. Sci.*, 2016, **133**, 43885.
- A. Reife, H.S. Fremann, *Environmental Chemistry of Dyes and Pigments*, Wiley, New York, 1996.
- S. Ardizzone, G. Cappelletti, D. Meroni, F. Spadavecchia, *Chem. Commun.* 2011, **47**, 2640–2642.
- D. Meroni, L. Lo Presti, G. Di Liberto, M. Ceotto, R.G. Acres, K.C. Prince, R. Bellani, G. Soliveri, S. Ardizzone, *J. Phys. Chem. C*, 2017, **121**, 430.
- J. P. Pouget, M. E. Jozefowicz, A. J. Epstein, X. Tang, A. G. MacDiarmid, *Macromolecules*, 1991, **24**, 779.
- Y. Wei, X. Tang, Y. Sun, W. W. Focke, *J. Poly. Sci.*, **27**, 1989, 2385.
- Y. Wei, G.-W. Jang, Ch.-Ch. Chan, K. F. Hsuen, R. Hariharan, S. A. Patel, C. K. Whitecar, *J. Phys. Chem.*, **94**, 1990, 7716.
- Y. Wei, R. Hariharan, S. A. Patel, *Macromolecules*, **23**, 1990, 758.
- Y. Wei, K. F. Hsueh, G.-W. Jang, *Polymer*, **35**, 1994, 3572.
- P.C. Ramamurthy, A. N. Mallya, A. Joseph, W. R. Harrell, R. V. Gregory, *Polym. Eng. Sci.* 2012, **52**, 1821.
- C. Della Pina, Z. Capáková, A. Sironi, P. Humpolíček, P. Sába, E. Falletta, *International Journal of Polymeric Materials and Polymeric Biomaterials*, 2017, **66**, 132.